

# miR-214-3p Promotes ox-LDL-Induced Macrophages Ferroptosis and Inflammation via GPX4

Xueliang Pei<sup>1</sup>, Facai Cui<sup>2</sup>, Yu Chen<sup>3</sup>, Zhiyuan Yang<sup>1</sup>, Zhouliang Xie<sup>1</sup>, Yongjin Wen<sup>1</sup>

<sup>1</sup>Department of Cardiovascular Surgery, Fuwai Central China Cardiovascular Hospital, Zhengzhou, Henan, People's Republic of China; <sup>2</sup>Clinical Laboratory, Henan Provincial People's Hospital, Zhengzhou, Henan, People's Republic of China; <sup>3</sup>Department of Pathology, Affiliated Cancer Hospital of Zhengzhou University, Zhengzhou, Henan, People's Republic of China

Correspondence: Xueliang Pei, Department of Cardiovascular Surgery, Fuwai Central China Cardiovascular Hospital, No. 1 Fuwai Avenue, Zhengdong New District, Zhengzhou, Henan, People's Republic of China, Email m15515600510@163.com

**Purpose:** Atherosclerosis (AS) is a chronic inflammatory disease caused by the dysregulation of lipid metabolism. It has been established that oxidized low-density lipoprotein (ox-LDL)-induced macrophage inflammation and ferroptosis play important roles in AS. However, the mechanism by which ox-LDL induces inflammation in macrophages requires further investigation.

**Materials and Methods:** A foam cell model derived from ox-LDL-induced macrophages was constructed to study its mechanism of action. The levels of interleukin (IL)-6, IL-1 $\beta$ , and tumor necrosis factor (TNF)- $\alpha$  were evaluated using an Enzyme-Linked Immunosorbent Assay (ELISA). Oil Red O staining was used to detect intracellular lipid accumulation levels. Lactate dehydrogenase (LDH), malondialdehyde (MDA), reactive oxygen species (ROS), and Fe<sup>2+</sup> levels were assessed. Dual-luciferase and RNA-binding protein immunoprecipitation (RIP) experiments validated the binding relationship between microRNA (miR)-214-3p and glutathione peroxidase 4 (GPX4).

**Results:** The levels of IL-6, IL-1 $\beta$ , and TNF- $\alpha$  were significantly increased in ox-LDL-induced macrophages, accompanied by increased lipid accumulation, indicating the promotion of foam cell formation. Additionally, ox-LDL increased LDH, MDA, ROS, and Fe<sup>2+</sup>. The expression of miR-214-3p positively correlated with ox-LDL concentration in macrophages. Treatment with an miR-214-3p inhibitor reduces lipid accumulation, inflammatory responses, and ferroptosis in macrophages. Dual-luciferase and RIP experiments confirmed that miR-214-3p regulates GPX4 transcription. Silenced GPX4 reversed the inflammatory effects of the miR-214-3p inhibitor on ox-LDL-induced macrophages. Low GPX4 expression also increased lipid accumulation and ferroptosis in macrophages.

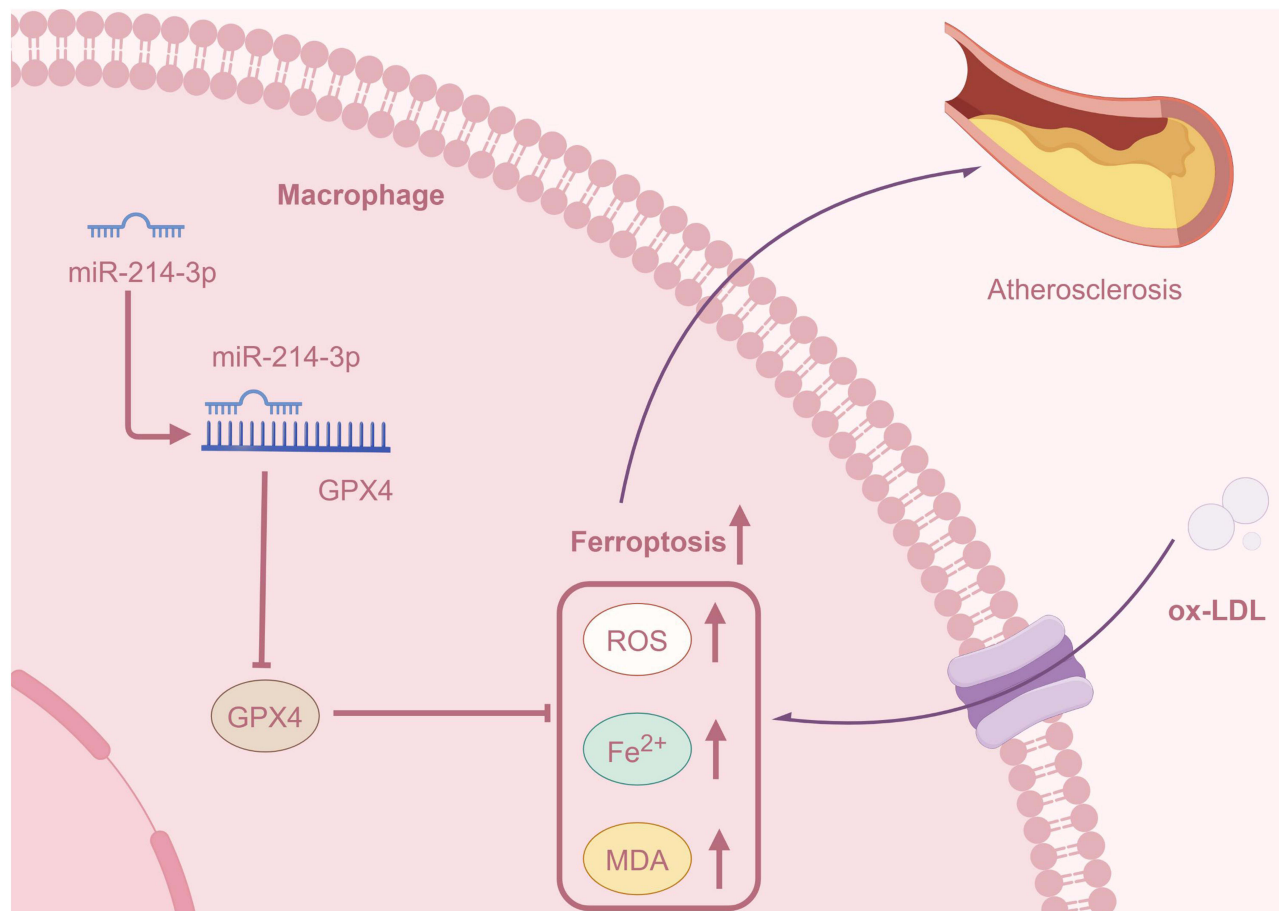
**Conclusion:** miR-214-3p promotes macrophage ferroptosis and inflammation induced by ox-LDL. This mechanism may be associated with miR-214-3p-induced GPX4 expression, which underscores the therapeutic significance of targeting macrophage inflammation and ferroptosis in addressing AS.

**Keywords:** atherosclerosis, ox-LDL, miR-214-3p, ferroptosis, inflammation, macrophages

## Introduction

Atherosclerosis (AS) is a chronic inflammatory disease characterized by the retention of atheroprone lipoproteins and accumulation of monocyte-derived macrophages triggering maladaptive immune response within the vessel wall of large arteries.<sup>1</sup> AS is widely acknowledged as a significant contributor to the pathogenesis of cardiovascular disease, leading to an annual mortality rate of approximately 610,000 individuals due to cardiac ailments in the United States.<sup>2</sup> Additionally, the incidence rate was higher in men than in women. It is worth noting that in recent years, the age of onset has been trending towards younger individuals, with early atherosclerotic lesions being detected in some young people.<sup>3</sup> The main cause of AS is currently believed to be lipid accumulation.<sup>4</sup> Low-density lipoprotein (LDL) and lipoprotein (a) (Lp(a)) can lead to AS.<sup>5</sup> Furthermore, the pathogenesis of AS can be influenced by comorbidities, such as hypertension, cardiovascular diseases, diabetes, and genetic predisposition.<sup>6</sup> As AS typically presents no obvious symptoms in its

## Graphical Abstract



early stages and symptoms in different organs vary post-onset, diagnosing the condition poses a certain challenge. Therefore, comprehensive exploration of the pathogenesis of AS is imperative to facilitate early detection and treatment strategies.

Macrophages are essential for the formation of AS. Early research has shown a close relationship between LDL and macrophages, contributing to the occurrence of AS.<sup>7</sup> The pathogenesis of AS is a multifaceted process encompassing sequential events including endothelial cell damage, lipid deposition, inflammatory reactions, and plaque formation.<sup>8</sup> Macrophages are one of the most important cell types in this process. In the early stages of AS, lipids deposit in the arterial wall to form lipid plaques, followed by activation of inflammatory responses.<sup>9</sup> Macrophages are attracted to damaged sites, where they engulf oxidized LDL (ox-LDL) particles, transform into foam cells, and subsequently form the core of plaques.<sup>10</sup> Apart from engulfing oxidized LDL particles, macrophages also participate in regulating inflammatory responses and releasing inflammatory mediators, thereby facilitating plaque initiation and progression.<sup>11</sup> Furthermore, macrophages can also induce the proliferation of vascular smooth muscle cells (VSMCs) and deposition of fibers within plaques, thereby accelerating plaque formation.<sup>12</sup> Therefore, AS progression is intricately linked to macrophage activity. Controlling macrophage activity may aid in the prevention and treatment of AS. However, the specific mechanism by which ox-LDL induces macrophage inflammation is not fully understood. Numerous studies have revealed that macrophage ferroptosis contributes significantly to AS.<sup>13,14</sup> Oxidative damage to phospholipids causes ferroptosis, an iron-dependent type of cell death that increases lipid peroxidation and compromises endothelial function, thereby promoting AS.<sup>14</sup> Additionally, disordered intracellular iron damages macrophages, VSMCs, and vascular endothelial cells (VECs),

affecting various risk factors and pathological processes associated with AS.<sup>15</sup> Despite these promising findings, further investigations are needed to elucidate the detailed mechanism of ox-LDL-induced macrophage ferroptosis.

MicroRNAs (miRNAs) are a class of non-coding RNAs capable of modulating cell function and biological processes through the regulation of gene expression.<sup>16</sup> Studies have demonstrated that miRNAs contributed a crucial role in AS, participating in regulating plaque formation and development by influencing lipid metabolism, inflammatory responses, cell proliferation, migration, and other aspects, which could affect the pathological progression of AS.<sup>6,17</sup> However, different miRNAs exhibit varying effects. miR-16-5p, which was derived from macrophage exosomes, promoted inflammatory responses and oxidative stress, exacerbating the pathological progression of AS.<sup>18</sup> Additionally, macrophage-derived exosomes expedite AS by promoting VSMC migration and proliferation via miR-21-3p/ phosphatase and tensin homolog (PTEN) mediation.<sup>19</sup> Conversely, miR-22-3p mitigated AS by regulating macrophage M2 polarization and nucleotide-binding oligomerisation domain-like receptor family pyrin domain containing 3 (NLRP3) activation.<sup>20</sup> miR-24 reduces the expression of matrix metalloproteinase (MMP)-14, thereby inhibiting macrophage invasion and alleviating AS.<sup>21</sup> Our previous study revealed that cancer susceptibility candidate 7 (CASC7) regulated the pathological progression of ox-LDL-stimulated AS cell models by modulating the miR-21/phosphatidylinositol 3-kinase (PI3K)/ protein kinase B (AKT) axis.<sup>22</sup> Recently, knocking down circular (Circ)\_0029589 suppressed VSMC malignant phenotype in response to ox-LDL exposure through the regulation of miR-214-3p and stromal interaction molecule 1 (STIM1).<sup>23</sup> Nevertheless, nothing is known about miR-214-3p's role in macrophages. Our knowledge of AS will improve with more research into the role and precise mechanism of miR-214-3p in mediating ox-LDL-induced macrophage inflammatory responses.

In this study, we initially detected how ox-LDL affects macrophages and discovered that it may encourage lipid buildup and an inflammatory response in these cells. In macrophages, ferroptosis is triggered by ox-LDL. Remarkably, the level of miR-214-3p increased markedly within macrophages following ox-LDL treatment in a dose-dependent manner. Building on these discoveries, we created cell models with low expression levels of miR-214-3p to examine its function in ox-LDL-induced macrophage pathways.

## Materials and Methods

### Cell Culture

THP-1 and HEK293T cells were obtained from American Type Culture Collection (ATCC, Manassas, VA, USA). THP-1 cells were grown in Roswell Park Memorial Institute (RPMI)-1640 medium (Gibco, Grand Island, NY, USA) supplemented with 1% penicillin-streptomycin (Gibco) and 10% fetal bovine serum (FBS, Gibco). The culture was maintained at 37°C with 5% CO<sub>2</sub>. HEK293T cells were grown in Gibco's DMEM supplemented with 10% FBS, 1% penicillin-streptomycin, and 5% CO<sub>2</sub> at 37°C. After treatment with phorbol 12-myristate 13-acetate (PMA, 200 ng/mL; Sigma-Aldrich, St. Louis, MO, USA) for 48 h, THP-1 cells were differentiated into M0 macrophages. In this study, 50 mg/L ox-LDL (Peking Union-Biology, Beijing, China) was used to establish a foam cell model produced from macrophages.

### Cell Transfection

miR-214-3p inhibitor and negative control (NC inhibitor) were obtained from MedChem Express (Monmouth Junction, NJ, USA). miR-214-3p mimic, short hairpin (sh)-GPX4, and their respective control plasmids (NC mimic and sh-NC) were obtained from GenePharma (Shanghai, China). Log-phase macrophages were transfected with these plasmids using Lipofectamine 2000 (Invitrogen, Carlsbad, CA, USA) and then incubated for 48 hours.

### Biological Indicator

The expression of IL-6, IL-1 $\beta$ , and TNF- $\alpha$  was assessed using Enzyme-Linked Immunosorbent Assay (ELISA) kits (Nanjing Jiancheng, Nanjing, China), following the manufacturer's instructions. The levels of Fe<sup>2+</sup> were determined using a kit (Elabscience, Wuhan, China), following the manufacturer's instructions. Briefly, the cells were incubated in the dark for 30 min with a fluorescent probe, and the OD was detected at 575 nm using a microplate reader. The levels of lactate dehydrogenase (LDH) and malondialdehyde (MDA) were examined using kits (Nanjing Jiancheng). The

absorbance was recorded using a spectrophotometer (Thermo Fisher Scientific, Waltham, MA, USA). Briefly, for the LDH assay, the cell supernatant was collected and supplemented with matrix buffer and coenzyme I for 15 min. Then 2, 4-dinitrophenylhydrazine was added, followed by 15 min of incubation. Finally, 0.4 mol/L NaOH was added to detect the optical density (OD) value at 440 nm. For MDA, the TBA method was used to examine the absorbance of the cell supernatant at 532 nm.

### Quantitative Real-Time-PCR (qRT-PCR) Assay

Total RNAs was extracted using the TRIzol reagent (Thermo Fisher Scientific). The SuperScript II First-Strand cDNA Synthesis Kit (Invitrogen) was used for cDNA synthesis. SYBR Green Master Mix was used for PCR amplification on an ABI 7500 Real-Time PCR System (Applied Biosystems, Foster City, CA). The comparative  $2^{-\Delta\Delta CT}$  method was used to calculate the relative expression levels of the target genes. GAPDH and U6 served as loading controls. The primer sequences are provided as follows: miR-214-3p forward primer 5'-GACAGCAGGCACAGACA-3', reverse primer 5'-GTGCAGGGTCCGAG-3'. GPX4 forward primer 5'-GAGGCAAGACCGAAGTAACTAC-3', reverse primer 5'-CCGAAGTGGTTACACGGGAA-3'. Glyceraldehyde-3-phosphate dehydrogenase (GAPDH) forward primer 5'-AAGAAGGTGGTGAAGCAGG-3', reverse primer 5'-GAAGGTGGAAGAGAGTGGGGAGT-3'. U6 forward primer 5'-GCTTCGGCAGCACATATACTAAAAT-3', reverse primer 5'-CGCTTCACGAATTTGCGTGTTCAT-3'.

### Western Blot (WB) Assay

Proteins were collected using RIPA reagent (Beyotime Biotechnology, Shanghai, China). Protein levels were quantified in cells and extracted using the BCA assay (Beyotime Biotechnology). Briefly, 20 µg of protein was separated by polyacrylamide gel electrophoresis (Beyotime Biotechnology) and transferred onto a polyvinylidene difluoride (PVDF) membrane (Beyotime Biotechnology). After blocking for 2 h with 5% skim milk, the samples were incubated with primary and secondary antibodies (1:1000, CST, Danvers, MA, USA). Finally, the cells were observed using an enhanced chemiluminescence (ECL) assay kit (Beo Tianmei Biotechnology, Shanghai, China). The antibodies used were as follows: GPX4 (1:1000, Abcam, UK) and GAPDH (1:1000, Abcam).

### The Levels of Reactive Oxygen Species (ROS)

ROS levels were measured using a commercial kit (Invitrogen). The cells were treated with 10 µM DCFH-DA solution and incubated for 20 min at 37°C. Next, serum-free media were used to wash the cells. A fluorescent microscope was used to monitor ROS concentrations.

### Oil Red O Staining

The cells were fixed with methyl alcohol for 10 min. An Oil Red O staining kit (Invitrogen) was used to detect lipid accumulation. The cells were stained with an Oil Red O staining solution for 20 min. The images were examined and captured using a microscope.

### Dual-Luciferase Assay

Wild-type (WT) or mutant (MUT) GPX4 3'UTR sequences were synthesized and cloned into the pmirGLO vector (Youbio, Shanghai, China) individually. HEK293T cells were seeded in a 24-well plate and co-transfected with either WT or MUT GPX4 plasmids, along with miR-214-3p mimics or NC mimics. After 48 h of transfection, cells were lysed and luciferase activity was measured using the Dual-Luciferase Reporter Assay System (Promega, Madison, Wisconsin, USA).

### RNA Binding Protein Immunoprecipitation (RIP)

To understand the binding relationship between miR-214-3p and GPX4, RIP experiments were performed. Magnetic bead-antibody complexes were first prepared using protein A/G agarose beads (Thermo Fisher Scientific) and GPX4 antibody (Abcam). The cells treated as indicated were lysed and immunoprecipitated. Purified RNA was examined by qRT-PCR after washing with phosphate buffered saline.



## Statistical Analysis

The experiment was conducted three times, and the quantitative data are expressed as the means  $\pm$  standard deviations. Statistical analysis and graphing were performed using SPSS-17.0 (IBM Corporation, Chicago, Illinois, USA) and GraphPad Prism-8.0 software (GraphPad Software, Inc., La Jolla, CA, USA), respectively. A *t* test (two groups) was used for two-group comparisons, and one-way analysis of variance (ANOVA) followed by the post hoc Tukey's test was used for multiple-group comparisons. Statistical significance was set at  $P < 0.05$ .

## Results

### ox-LDL Induced Lipid Accumulation, Inflammation and Ferroptosis in Macrophages

Foam cell formation derived from macrophages is an early sign of atherosclerotic lesions. PMA was used to induce differentiation of THP-1 cells into M0 macrophages. Subsequently, a foam cell model derived from macrophages was developed by exposing cells to 50 mg/L ox-LDL. Initially, we detected a notable increase in IL-6, IL-1 $\beta$ , and TNF- $\alpha$  levels in the macrophage supernatant after ox-LDL treatment, as confirmed by ELISA and qRT-PCR (Figure 1A and B). These data indicate that an inflammatory response is induced by ox-LDL. Oil Red O staining revealed a notable elevation in lipid accumulation in macrophages after ox-LDL treatment (Figure 1C). Furthermore, the ox-LDL group showed higher ROS activity than the control group (Figure 1D). Intracellular LDH and MDA levels displayed a similar trend (Figure 1E and F). Importantly, we found a significant increase in intracellular Fe<sup>2+</sup> levels (Figure 1G). These results revealed that ox-LDL induces lipid accumulation, inflammation, and ferroptosis in macrophages, leading to the formation of foam cells.

### Downregulation of miR-214-3p Mitigated ox-LDL-Induced Lipid Accumulation and Inflammation in Macrophages

To investigate the specific mechanism by which ox-LDL induced foam cell formation in macrophages, we treated macrophages with 0, 25, 50, 100, or 200 mg/L ox-LDL. Notably, miR-214-3p levels increased with increasing concentrations of ox-LDL (Figure 2A). Subsequently, we constructed a low expression miR-214-3p cell line. A significant reduction in miR-214-3p expression in the miR-214-3p inhibitor group compared to that in the control group confirmed the successful establishment of the miR-214-3p knockdown cell line (Figure 2B). The administration of ox-LDL to downregulated macrophages of miR-214-3p resulted in a substantial decrease in the inflammatory response (IL-6, IL-1 $\beta$ , and TNF- $\alpha$  levels) in macrophages when compared to the ox-LDL + NC inhibitor group. This suggests that miR-214-3p inhibitors were effective in suppressing inflammation (Figure 2C and D). Additionally, Oil Red O staining results indicated that the miR-214-3p inhibitor decreased the quantity of lipid buildup induced by ox-LDL in macrophages (Figure 2E).

### The Downregulation of miR-214-3p Alleviates ox-LDL-Induced Macrophages Ferroptosis

Additional research on the effect of miR-214-3p on ox-LDL showed that when macrophages were treated with ox-LDL, low levels of miR-214-3p decreased ROS activity (Figure 3A). The detection of intracellular LDH and MDA levels showed a significant reduction after treatment with the miR-214-3p inhibitor compared to the NC inhibitor (Figure 3B and C). Additionally, the data indicated that Fe<sup>2+</sup> levels in macrophages treated with the miR-214-3p inhibitor and ox-LDL were suppressed (Figure 3D). These findings indicate that downregulation of miR-214-3p inhibits ox-LDL-induced ferroptosis in macrophages.

### miR-214-3p Inhibits the Transcription of GPX4

To further explore how miR-214-3p enhances the action of ox-LDL, we conducted bioinformatics analysis, revealing binding sites between miR-214-3p and GPX4 (Figure 4A). An miR-214-2p mimic cell line was constructed (Figure 4B). Dual-luciferase experiment results demonstrated that the luciferase activity of wild-type GPX4 was significantly decreased following overexpression of miR-214-3p, whereas the luciferase activity of mutant GPX4 showed no change (Figure 4C).

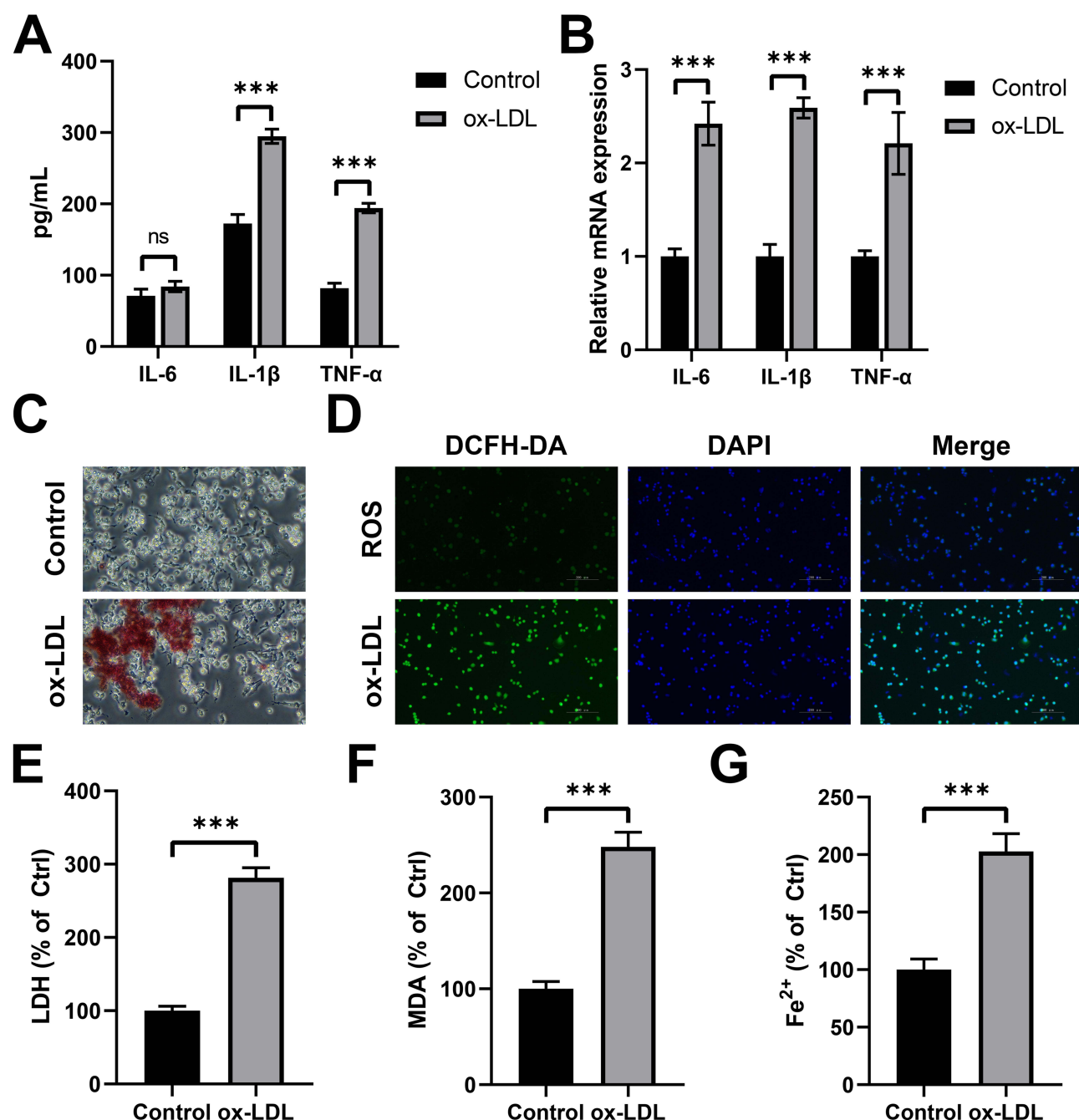


**Figure 1** ox-LDL induced lipid accumulation, inflammation and ferroptosis in macrophages. (A) The levels of IL-6, IL-1 $\beta$  and TNF- $\alpha$  in macrophages using ELISA assay. (B) The expression of IL-6, IL-1 $\beta$  and TNF- $\alpha$  in macrophages using qRT-PCR assay. (C) The levels of lipid accumulation in macrophages. (D) The activity of ROS in macrophages. (E) The levels of LDH in macrophages. (F) The levels of MDA in macrophages. (G) The levels of Fe<sup>2+</sup> in macrophages. (ns, not significant, \*\*\* $P < 0.001$ ).

Furthermore, the RIP results showed a binding relationship between miR-214-3p and GPX4 (Figure 4D). These findings demonstrate that miR-214-3p regulates the expression of GPX4. Based on these data, the addition of an miR-214-3p inhibitor increased GPX4 mRNA levels in the model group (Figure 4E). The protein levels of GPX4 showed a similar trend. Exposure of ox-LDL-induced macrophages to low levels of miR-214-3p prevented the downregulation of GPX4 (Figure 4F).

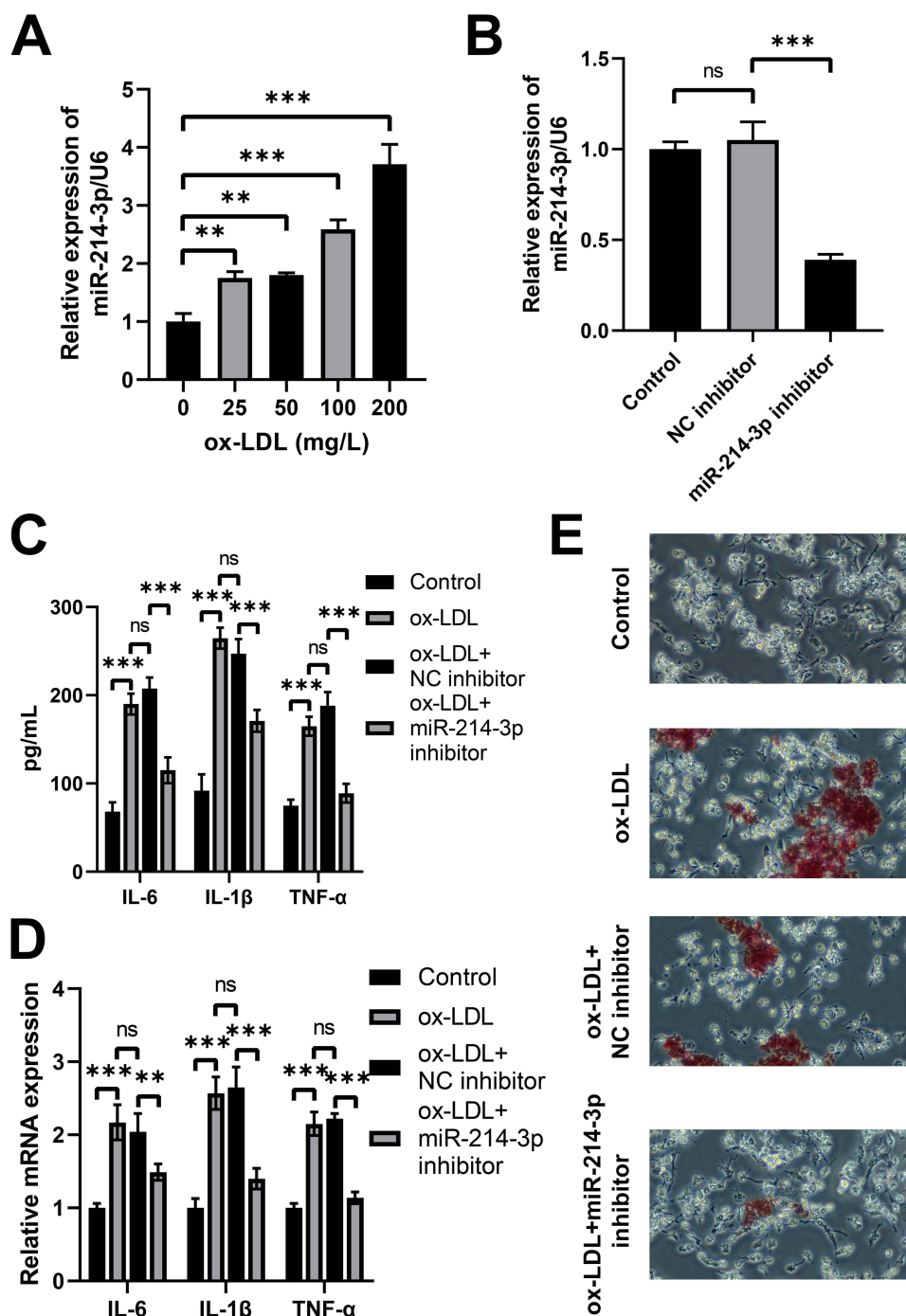


**Figure 2** The downregulation of miR-214-3p alleviates ox-LDL-induced lipid accumulation and inflammation in macrophages. (A) The levels of miR-214-3p in macrophages treated with ox-LDL. (B) The expression of miR-214-3p in macrophages treated with miR-214-3p inhibitor. (C) The levels of IL-6, IL-1 $\beta$  and TNF- $\alpha$  in macrophages using ELISA assay. (D) The levels of IL-6, IL-1 $\beta$  and TNF- $\alpha$  in macrophages using qRT-PCR assay. (E) The levels of lipid accumulation in macrophages. (ns, not significant, \*\* $P < 0.01$ , \*\*\* $P < 0.001$ ).

## miR-214-3p Regulates Lipid Accumulation and Inflammation in ox-LDL-Induced Macrophages by Targeting GPX4

Next, we constructed sh-GPX4 cell lines. qRT-PCR and WB data revealed a marked reduction in both mRNA and protein levels after treatment with the sh-GPX4 plasmid (Figure 5A and B). The cells were divided into control, ox-LDL, ox-LDL + miR-214-3p inhibitor, ox-LDL + miR-214-3p inhibitor + sh-NC, and ox-LDL + miR-214-3p inhibitor + sh-GPX4 groups. The ELISA

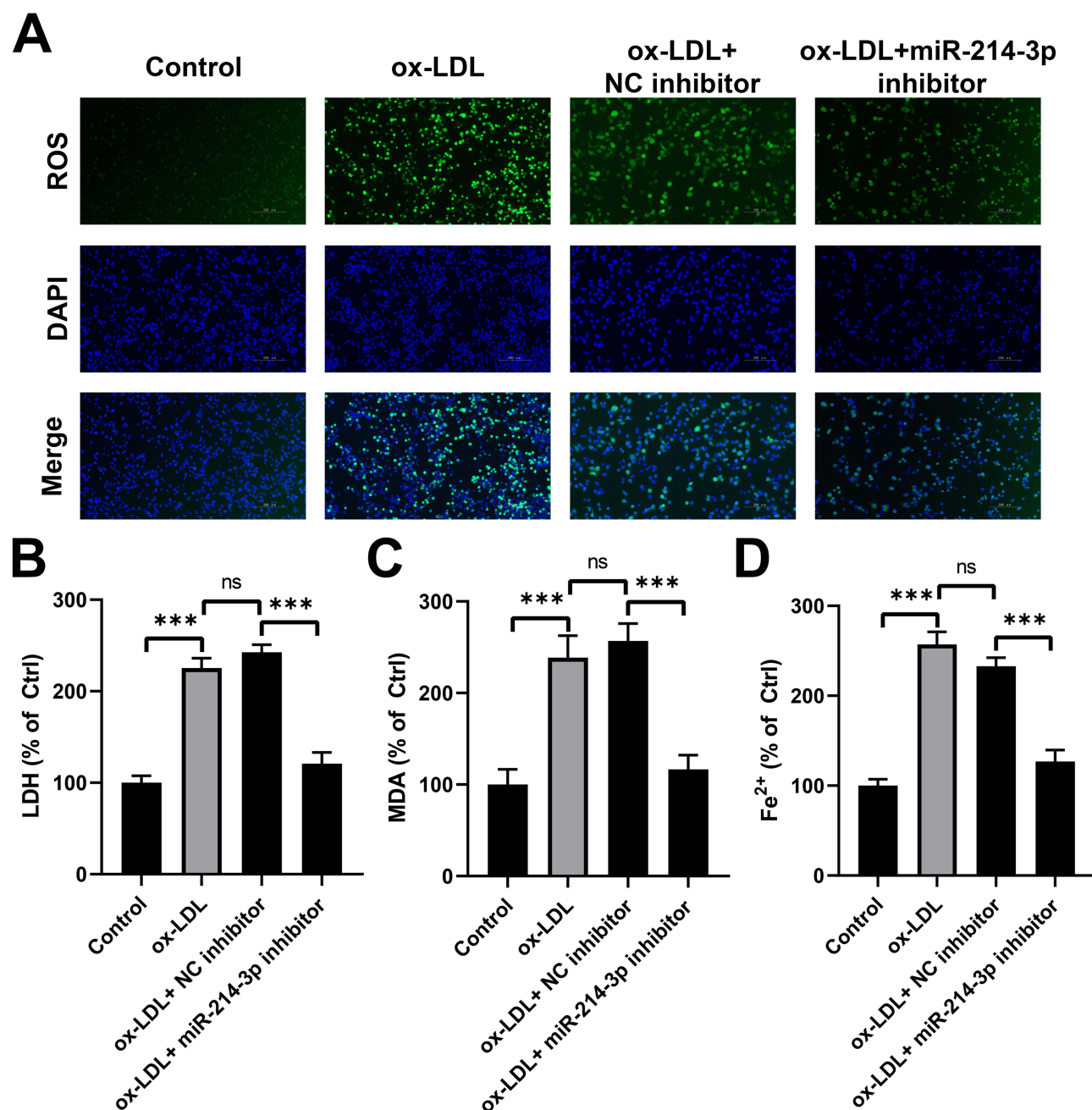


**Figure 3** The downregulation of miR-214-3p alleviates ox-LDL-induced ferroptosis in macrophages. **(A)** The activity of ROS in macrophages. **(B)** The levels of LDH in macrophages. **(C)** The levels of MDA in macrophages. **(D)** The levels of Fe<sup>2+</sup> in macrophages. (ns, not significant, \*\*\**P* < 0.001).

results showed an increase in IL-6, IL-1 $\beta$ , and TNF- $\alpha$  levels after inhibiting the expression of GPX4 in ox-LDL-induced macrophages (Figure 5C). The substantial elevation of TNF- $\alpha$ , IL-1 $\beta$ , and IL-6 expression was also verified by qRT-PCR (Figure 5D), which indicated that silencing GPX4 reversed the inflammatory inhibitory effect of miR-214-3p inhibitor on ox-LDL-induced macrophages. Additionally, Oil Red O staining results corroborated an increase in intracellular lipid accumulation levels in ox-LDL-induced miR-214-3p and GPX4 knocked-macrophages, indicating that silencing GPX4 attenuated the inhibition of miR-214-3p in ox-LDL-induced macrophages (Figure 5E).

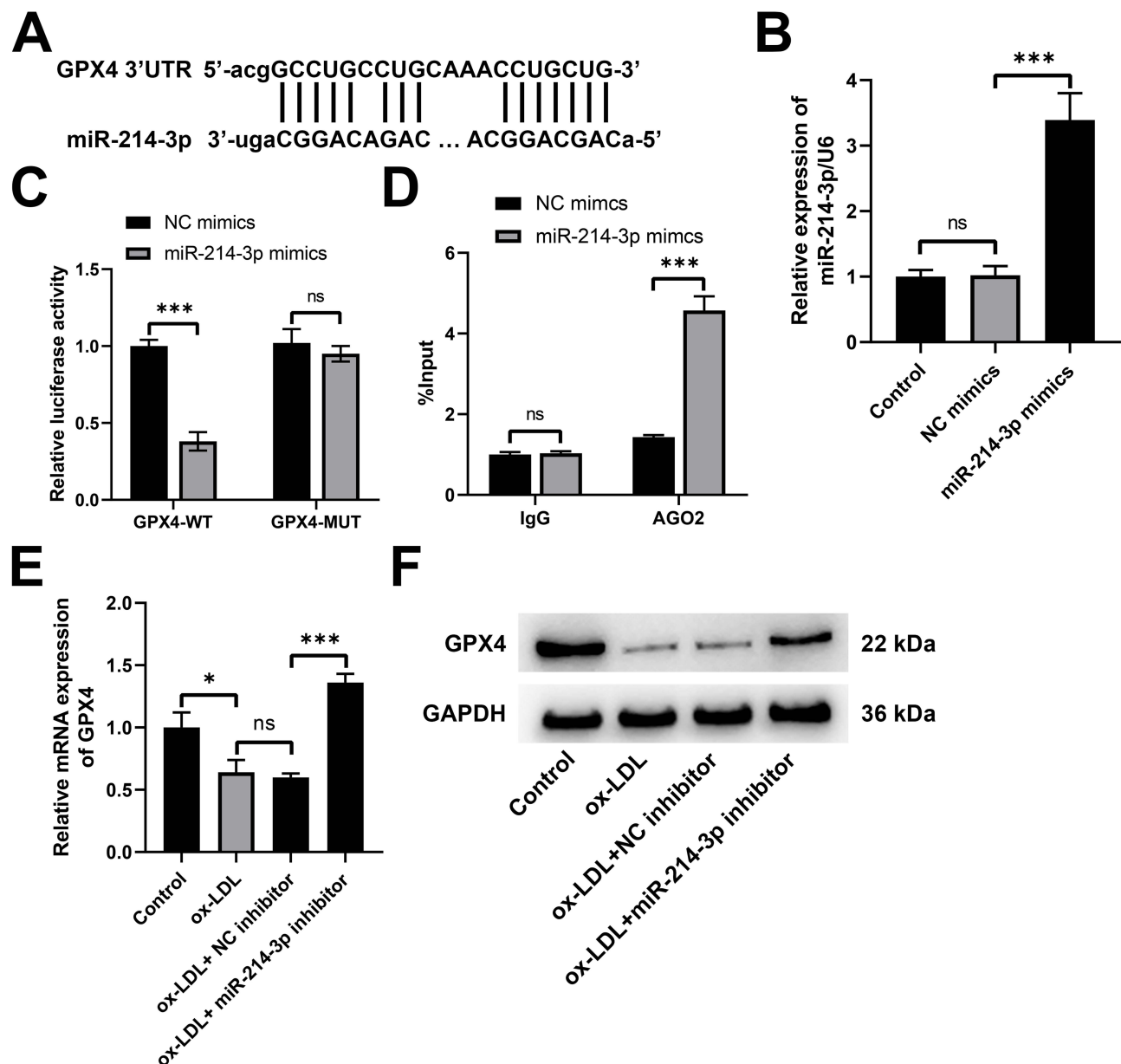
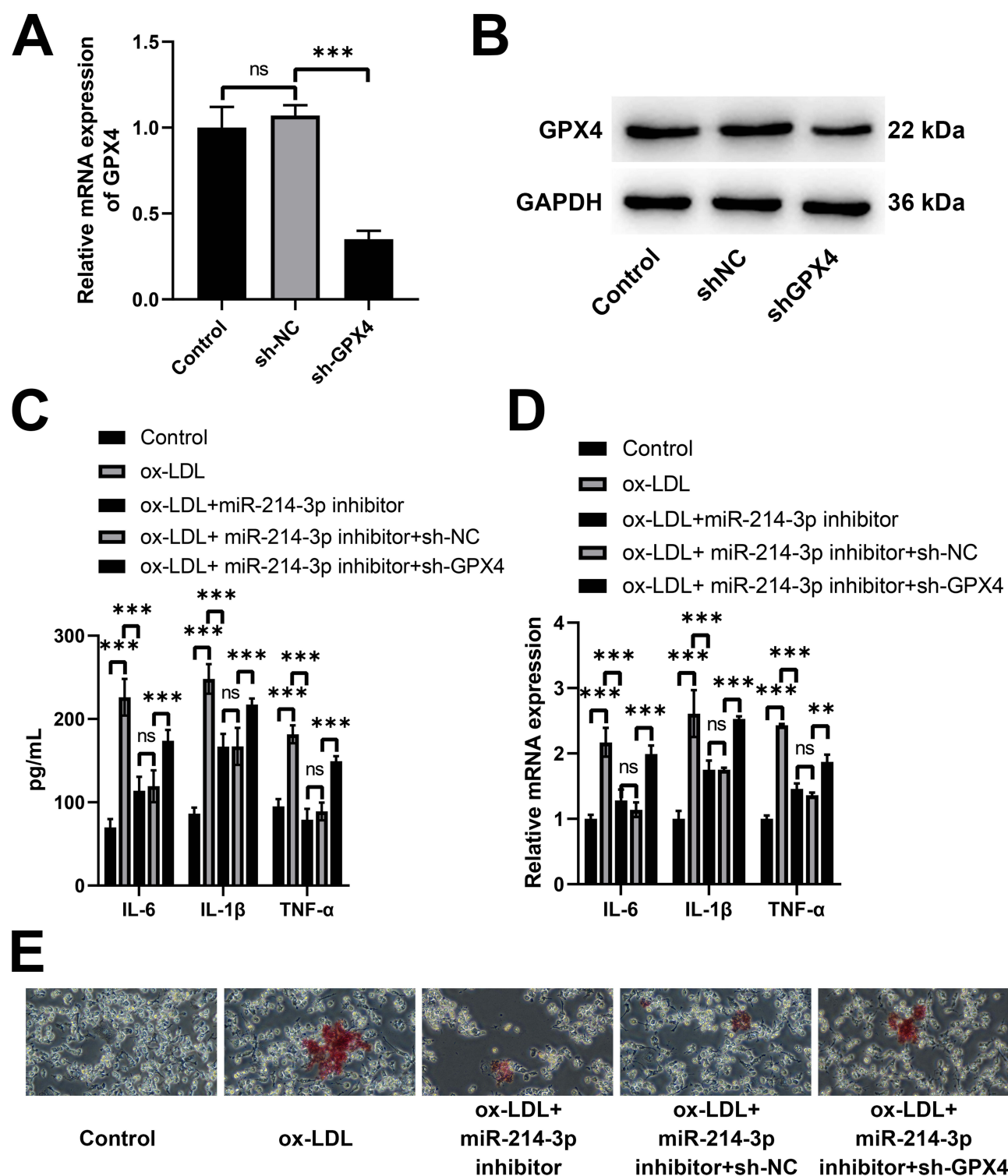


**Figure 4** miR-214-3p inhibits the transcription of GPX4. (A) The binding sites between miR-214-3p and GPX4 using bioinformatics analysis. (B) miR-214-3p expression levels in macrophages were increased following transfection with miR-214-3p mimic. (C) Luciferase reporter assays showing that miR-214-3p interacts with the 3'UTR of GPX4. (D) RIP assays showed a direct interaction between miR-214-3p and GPX4. (E) The mRNA levels of GPX4 were examined by qRT-PCR assay. (F) The protein levels of GPX4 were examined by WB assay. (ns, not significant, \* $P < 0.05$ , \*\*\* $P < 0.001$ ).

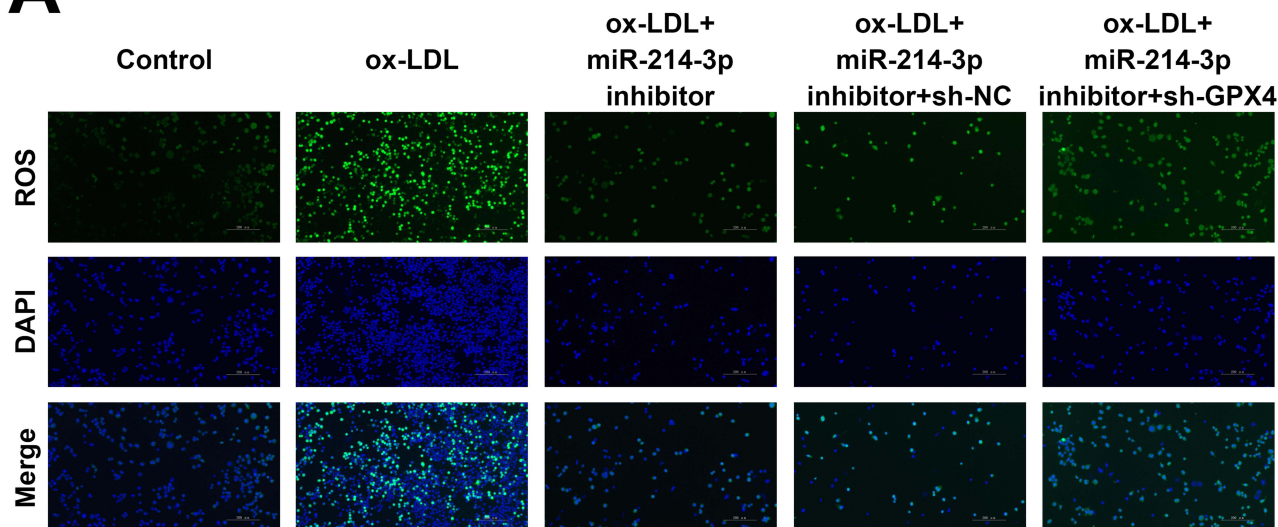
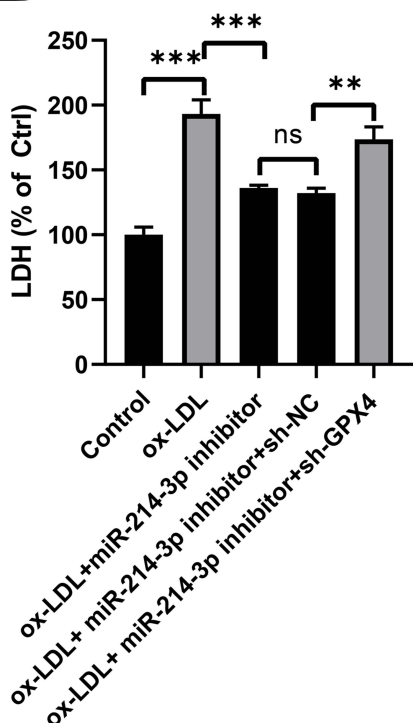
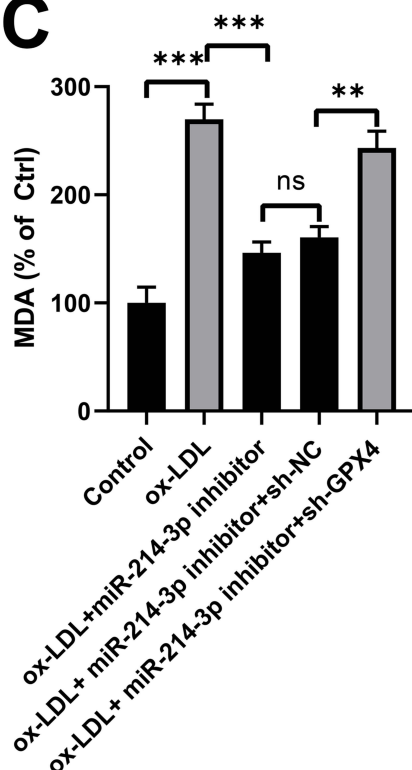
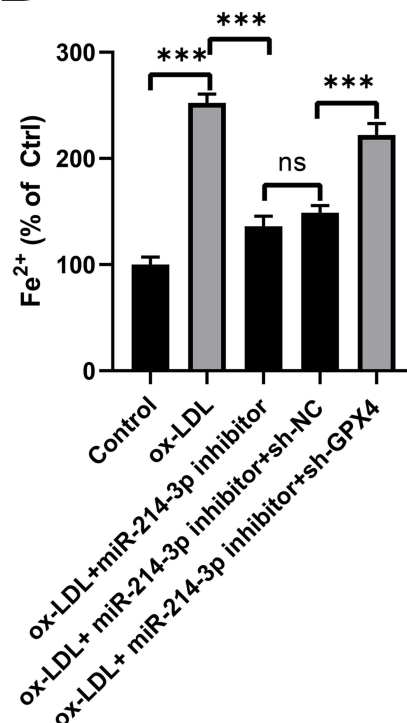
## miR-214-3p Regulates ox-LDL-Induced Macrophages Ferroptosis via GPX4

Importantly, in the ox-LDL + miR-214-3p inhibitor + sh-GPX4 group, ROS activity was significantly increased compared to that in the ox-LDL + miR-214-3p inhibitor + sh-NC group (Figure 6A). The levels of LDH and MDA within the cells also showed a similar trend, with a significant elevation in LDH and MDA levels in GPX4 silenced cells after the introduction of ox-LDL and miR-214-3p inhibitor (Figure 6B and C). Furthermore, we found a significant increase in  $Fe^{2+}$  levels after silencing GPX4 (Figure 6D). Collectively, these data indicate that miR-214-3p induces ferroptosis in macrophages by inhibiting GPX4.





**Figure 5** miR-214-3p regulates lipid accumulation and inflammation in ox-LDL-induced macrophages via targeting GPX4. (A) The mRNA levels of GPX4 were examined by qRT-PCR assay. (B) The protein levels of GPX4 were examined by WB assay. (C) The levels of IL-6, IL-1β and TNF-α in macrophages were examined by ELISA assay. (D) The expression levels of IL-6, IL-1β and TNF-α in macrophages were examined by qRT-PCR assay. (E) The levels of lipid accumulation in macrophages. (ns, not significant, \*\* $P < 0.01$ , \*\*\* $P < 0.001$ ).

**A****B****C****D**

**Figure 6** miR-214-3p inhibits GPX4 to regulate ox-LDL-induced macrophages ferroptosis. **(A)** The activity of ROS in macrophages. **(B)** The levels of LDH in macrophages. **(C)** The levels of MDA in macrophages. **(D)** The levels of Fe<sup>2+</sup> in macrophages. (ns, not significant, \*\**p* < 0.01, \*\*\**p* < 0.001).

## Discussion

Atherosclerosis is fundamentally characterized by chronic inflammatory responses in endothelial cells, macrophages, and smooth muscle cells.<sup>24</sup> In the early stages of atherosclerosis, the creation of foam cells produced from macrophages is essential for the development and rupture of atherosclerotic plaques. ox-LDL, as a key inducer of AS, could enhance the accumulation of macrophage-derived foam cells.<sup>10</sup> Current research has reported that macrophage-mediated inflammatory responses are involved in ferroptosis.<sup>25</sup> In our study, ox-LDL upregulated the levels of inflammatory factors in

macrophages. Additionally, ox-LDL increased lipid accumulation in macrophages. ox-LDL could promote the formation of macrophage foam cell models, thereby accelerating the progression of AS. Furthermore, ox-LDL increased the levels of ROS, LDH, MDA, and  $\text{Fe}^{2+}$ , which were consistent with the characteristics of ferroptosis and consistent with the results of You et al.<sup>13</sup> These results suggested an association between ox-LDL and macrophage ferroptosis.

Based on the macrophage-derived foam cell model, we examined miR-214-3p expression. Interestingly, with increasing concentrations of ox-LDL, the expression of miR-214-3p gradually increased, which indicated that up-regulation of miR-214-3p in macrophages promoted foam cell formation. miR-214-3p could mediate the pathogenesis of AS by regulating ox-LDL-induced autophagy in HUVECs, which was attributed to its binding to the 3' UTR of ATG5.<sup>26</sup> miR-214-3p was found to facilitate the malignant progression and inflammation of HVMSCs by regulating forkhead box O 1 (FOXO1) in an ox-LDL-induced AS in vitro model.<sup>27</sup> In the present study, we also proved that down-regulation of miR-214-3p levels effectively alleviated the increase in inflammatory factors and lipid accumulation induced by ox-LDL in macrophages. In addition, previous reports have found that miR-214-3p could induce ferroptosis in a variety of cells. He et al proved that the miR-214-3p could accelerated the ferroptosis of live cancer cells.<sup>28</sup> Inhibition of miR-214-3p has also been shown to attenuate ferroptosis in myocardial infarction.<sup>29</sup> Recent studies have also found that miR-214-3p could inhibit lipopolysaccharide (LPS)-induced macrophage inflammation and attenuates the progression of dry eye syndrome by regulating ferroptosis in cells.<sup>30</sup> Importantly, we also found that low expression of miR-214-3p significantly repressed ROS activity, LDH, MDA, and  $\text{Fe}^{2+}$  levels induced by ox-LDL in macrophages. These findings indicate that low miR-214-3p expression can inhibit ox-LDL-induced macrophage ferroptosis.

In the present study, we further elucidated the involvement of miR-214-3p in ox-LDL-induced macrophage ferroptosis. Interestingly, we found that GPX4 and miR-214-3p have potential binding sites. Importantly, miR-214-3p could regulate the transcription levels of GPX4. As an intracellular antioxidant enzyme, GPX4 scavenges lipid oxygenase and neutralizes lipid peroxides to prevent ferroptosis.<sup>31,32</sup> Additionally, in concert with the antioxidant glutathione, GPX4 catalyzes the reduction of hydrogen peroxide and organic hydroperoxides (GSH).<sup>33</sup> When GPX4 is inactivated or knocked down, lipid peroxides accumulate, triggering ferroptosis and accelerating the development of AS.<sup>34,35</sup> GPX4 overexpression may reduce lipid peroxidation and prevent AS progression. As anticipated, we discovered that the GPX4 levels in macrophages were much greater than that in the model group after treatment with ox-LDL and miR-214-3p inhibitors. This implies that to support the inflammatory response and ferroptosis of ox-LDL-induced macrophages, miR-214-3p probably controls GPX4 expression.

To validate this hypothesis, we inhibited both miR-214-3p and GPX4 expression levels in ox-LDL-induced macrophages. Compared to sh-NC cells, the expression of IL-1 $\beta$ , IL-6, and TNF- $\alpha$  in GPX4 silenced macrophages co-treated with ox-LDL and miR-214-3p inhibitor was upregulated, indicating that silencing GPX4 weakened the inhibitory effect of the miR-214-3p inhibitor on the inflammatory response of ox-LDL-induced macrophages. Additionally, silencing GPX4 weakened the inhibitory effect of the miR-214-3p inhibitor on lipid accumulation in ox-LDL-induced macrophages. Co-treatment of GPX4 macrophages with miR-214-3p inhibitor and ox-LDL, further validation of ferroptosis-related indicators, showed that ROS activity and the levels of LDH, MDA, and  $\text{Fe}^{2+}$  were considerably elevated. Our results suggest a role for GPX4 in the ferroptosis of ox-LDL-induced macrophages, which was influenced by miR-214-3p. By downregulating GPX4, miR-214-3p facilitated the ferroptosis of ox-LDL-induced macrophages. Extensive literatures have also proved that GPX4 was regulated by a variety of miRNAs. Overexpression of miR-132 decreased the GPX4 to exacerbate AS.<sup>36</sup> miR-17-92 has also been proposed as a potent target for regulating ferroptosis, which up-regulated GPX4 expression via A20-ACSL4 axis to alleviate HUVEC ferroptosis.<sup>37</sup> Nevertheless, there are certain limitations that require further research. Additional in vivo validation of miR-214-3p's function is required. In addition to GPX4, miRNAs may regulate macrophage ferroptosis via other mechanisms.

The present study had certain limitations that should be acknowledged. First, although we investigated the potential role of miR-214-3p in human cell models, in vivo experiments should be performed to confirm whether this effect also exists in animal models. Collecting and analyzing more tissue samples would enhance the generalizability of the conclusions. In addition, there are many ferroptosis targets of AS that can be further analyzed to determine the effects of other targets on macrophage ferroptosis and inflammation in AS. Finally, the results of this study also need to be

verified by using clinical samples of AS patients in the future to clarify the association between miR-214-3p and the disease course of AS patients.

## Conclusion

In conclusion, our results elucidate the connection between inflammation and ferroptosis in ox-LDL-induced macrophages. The putative therapeutic target miR-214-3p stimulates inflammation and ferroptosis of macrophages generated by ox-LDL. Moreover, miR-214-3p promotes macrophage ferroptosis by downregulating GPX4, and silencing GPX4 restores this effect. These results provide a new perspective for exploring the molecular mechanisms of ferroptosis in AS and a new therapeutic target for treating AS patients.

## Abbreviations

AS, Atherosclerosis; ox-LDL, oxidized low-density lipoprotein; IL, Interleukin; TNF, Tumor necrosis factor; ELISA, Enzyme-Linked Immunosorbent Assay; LDH, Lactate dehydrogenase; MDA, Malondialdehyde; ROS, Reactive oxygen species; RIP, RNA-binding protein immunoprecipitation; miR, microRNA; GPX4, Glutathione peroxidase 4; Lp(a), Lipoprotein (a); VSMCs, Vascular smooth muscle cells; VECs, Vascular endothelial cells; PTEN, Phosphatase and tensin homolog; NLRP3, nucleotide-binding oligomerisation domain-like receptor family pyrin domain containing 3; MMP, matrix metalloproteinase; CASC7, cancer susceptibility candidate 7; PI3K, phosphatidylinositol 3-kinase; AKT, Protein kinase B; Circ, circular; STIM1, Stromal interaction molecule 1; ATCC, American Type Culture Collection; RPMI, Roswell Park Memorial Institute; FBS, Fetal bovine serum; PMA, Phorbol 12-myristate 13-acetate; sh, short hairpin; NC, Negative control; OD, optical density; qRT-PCR, Quantitative Real-time-PCR; GAPDH, glyceraldehyde-3-phosphate dehydrogenase; WB, Western blot; PVDF, polyvinylidene difluoride; ECL, enhanced chemiluminescence; WT, Wild-type; MUT, Mutant; GSH, glutathione; ANOVA, One-way analysis of variance; LPS, Lipopolysaccharide; FOXO1, Forkhead box O 1.

## Data Sharing Statement

All the results are presented in the article. Further inquiries can be directed to the corresponding authors.

## Disclosure

The authors report no conflicts of interest in this work.

## References

1. Tabas I, Bornfeldt KE. Macrophage phenotype and function in different stages of atherosclerosis. *Cir Res*. 2016;118(4):653–667. doi:10.1161/circresaha.115.306256
2. Volgman AS, Palaniappan LS, Aggarwal NT, et al. Atherosclerotic cardiovascular disease in South Asians in the United States: epidemiology, risk factors, and treatments: a scientific statement from the American Heart Association. *Circulation*. 2018;138(1):e1–e34. doi:10.1161/cir.0000000000000580
3. Libby P. The changing landscape of atherosclerosis. *Nature*. 2021;592(7855):524–533. doi:10.1038/s41586-021-03392-8
4. Cao H, Jia Q, Yan L, Chen C, Xing S, Shen D. Quercetin suppresses the progression of atherosclerosis by regulating MST1-mediated autophagy in ox-LDL-induced RAW264.7 macrophage foam cells. *Int J mol Sci*. 2019;20(23):6093. doi:10.3390/ijms20236093
5. Libby P. Inflammation in atherosclerosis. *Nature*. 2002;420(6917):868–874. doi:10.1038/nature01323
6. Jebari-Benslaiman S, Galicia-García U, Larrea-Sebal A, et al. Pathophysiology of atherosclerosis. *Int J mol Sci*. 2022 23(6) doi:10.3390/ijms23063346
7. Yokode M, Kita T. Macrophages and arteriosclerosis. *Nihon Naika Gakkai zasshi*. 1994 83(9):1520–1525.
8. Fan J, Watanabe T. Atherosclerosis: known and unknown. *Pathol Int*. 2022;72(3):151–160. doi:10.1111/pin.13202
9. Zhu Y, Xian X, Wang Z, et al. Research progress on the relationship between atherosclerosis and inflammation. *Biomolecules*. 2018;8(3):80. doi:10.3390/biom8030080
10. Wang T, Lu H. Ganoderic acid A inhibits ox-LDL-induced THP-1-derived macrophage inflammation and lipid deposition via notch1/PPARγ/CD36 signaling. *Adv Clin Exp Med*. 2021;30(10):1031–1041. doi:10.17219/acem/137914
11. Chistiakov DA, Melnichenko AA, Myasoedova VA, Grechko AV, Orekhov AN. Mechanisms of foam cell formation in atherosclerosis. *J Mol Med*. 2017;95(11):1153–1165. doi:10.1007/s00109-017-1575-8
12. Yurdagül A Jr. Crosstalk between macrophages and vascular smooth muscle cells in atherosclerotic plaque stability. *Arterioscler Thromb Vasc Biol*. 2022;42(4):372–380. doi:10.1161/atvbaha.121.316233
13. You Z, Ye X, Jiang M, Gu N, Liang C. Inc-MRGPRF-6:1 promotes ox-LDL-INDUCED MACROPHAGE FERROPTOSIS VIA SUPPRESSING GPX4. *Mediators Inflamm*. 2023;2023:5513245. doi:10.1155/2023/5513245

14. Ma J, Zhang H, Chen Y, Liu X, Tian J, Shen W. The role of macrophage iron overload and ferroptosis in atherosclerosis. *Biomolecules*. 2022;12(11):1702. doi:10.3390/biom12111702
15. Ouyang S, You J, Zhi C, et al. Ferroptosis: the potential value target in atherosclerosis. *Cell Death Dis* 2021;12(8):782. doi:10.1038/s41419-021-04054-3
16. Lee YS, Dutta A. MicroRNAs in cancer. *Ann Rev Pathol*. 2009;4:199–227. doi:10.1146/annurev.pathol.4.110807.092222
17. Citrin KM, Fernández-Hernando C, Suárez Y. MicroRNA regulation of cholesterol metabolism. *Ann N Y Acad Sci* 2021;1495(1):55–77. doi:10.1111/nyas.14566
18. Chen F, Li J, She J, Chen T, Yuan Z. Exosomal microRNA-16-5p from macrophage exacerbates atherosclerosis via modulating mothers against decapentaplegic homolog 7. *Microvascular Res*. 2022;142:104368. doi:10.1016/j.mvr.2022.104368
19. Zhu J, Liu B, Wang Z, et al. Exosomes from nicotine-stimulated macrophages accelerate atherosclerosis through miR-21-3p/PTEN-mediated VSMC migration and proliferation. *Theranostics*. 2019;9(23):6901–6919. doi:10.7150/thno.37357
20. Bian X, Peng H, Wang Y, Guo H, Shi G. MicroRNA-22-3p alleviates atherosclerosis by mediating macrophage M2 polarization as well as inhibiting NLRP3 activation. *J Int Med Res*. 2023;51(10):3000605231197071. doi:10.1177/03000605231197071
21. Di Gregoli K, Jenkins N, Salter R, White S, Newby AC, Johnson JL. MicroRNA-24 regulates macrophage behavior and retards atherosclerosis. *Arterioscler Thromb Vasc Biol*. 2014;34(9):1990–2000. doi:10.1161/ATVBAHA.114.304088
22. Pei X, Wen Y, Cui F, Yang Z, Xie Z. lncRNA CASC7 regulates pathological progression of ox-LDL-stimulated atherosclerotic cell models via sponging miR-21 and regulating PI3K/Akt and TLR4/NF-kappaB signaling pathways. *Aging*. 2021;13(23):25408–25425. doi:10.18632/aging.203757
23. Huang Z, Li P, Wu L, et al. Hsa\_circ\_0029589 knockdown inhibits the proliferation, migration and invasion of vascular smooth muscle cells via regulating miR-214-3p and STIM1. *Life Sci*. 2020. 259. 118251. doi:10.1016/j.lfs.2020.118251
24. Rao C, Liu B, Huang D, et al. Nucleophosmin contributes to vascular inflammation and endothelial dysfunction in atherosclerosis progression. *J Thoracic Cardiovasc Surg*. 2021;161(5):e377–e393. doi:10.1016/j.jtcvs.2019.10.152
25. Luo L, Huang F, Zhong S, Ding R, Su J, Li X. Astaxanthin attenuates ferroptosis via Keap1-Nrf2/HO-1 signaling pathways in LPS-induced acute lung injury. *Life Sci*. 2022;311(Pt A):121091. doi:10.1016/j.lfs.2022.121091
26. Wang J, Wang WN, Xu SB, et al. MicroRNA-214-3p: a link between autophagy and endothelial cell dysfunction in atherosclerosis. *Acta Physiol*. 2018;222(3). doi:10.1111/apha.12973
27. Li X, Li L, Dong X, Ding J, Ma H, Han W. Circ\_GRN promotes the proliferation, migration, and inflammation of vascular smooth muscle cells in atherosclerosis through miR-214-3p/FOXO1 axis. *J Cardiovasc Pharmacol*. 2021;77(4):470–479. doi:10.1097/fjc.0000000000000982
28. He GN, Bao NR, Wang S, Xi M, Zhang TH, Chen FS. ketamine induces ferroptosis of liver cancer cells by targeting lncRNA PVT1/miR-214-3p/GPX4. *Drug Des Devel Ther*. 2021;15:3965–3978. doi:10.2147/dddt.S332847
29. Liu F, Jiang LJ, Zhang YX, et al. Inhibition of miR-214-3p attenuates ferroptosis in myocardial infarction via regulating ME2. *Biochem Biophys Res Commun*. 2023;661:64–74. doi:10.1016/j.bbrc.2023.04.031
30. Zhao D, Ji H, Zhang W, et al. miR-214-3p inhibits LPS-induced macrophage inflammation and attenuates the progression of dry eye syndrome by regulating ferroptosis in cells. *Genes Genomics*. 2025;47(2):183–195. doi:10.1007/s13258-024-01598-4
31. Yang WS, SriRamaratnam R, Welsch ME, et al. Regulation of ferroptotic cancer cell death by GPX4. *Cell*. 2014;156(1–2):317–331. doi:10.1016/j.cell.2013.12.010
32. Stockwell BR, Friedmann Angeli JP, Bayir H, et al. Ferroptosis: a regulated cell death nexus linking metabolism, redox biology, and disease. *Cell*. 2017;171(2):273–285. doi:10.1016/j.cell.2017.09.021
33. Ye Y, Chen A, Li L, et al. Repression of the antiporter SLC7A11/glutathione/glutathione peroxidase 4 axis drives ferroptosis of vascular smooth muscle cells to facilitate vascular calcification. *Kidney Int*. 2022;102(6):1259–1275. doi:10.1016/j.kint.2022.07.034
34. Feng H, Stockwell BR. Unsolved mysteries: how does lipid peroxidation cause ferroptosis? *PLoS Biol*. 2018;16(5):e2006203. doi:10.1371/journal.pbio.2006203
35. Ma T, Du J, Zhang Y, Wang Y, Wang B, Zhang T. GPX4-independent ferroptosis-a new strategy in disease's therapy. *Cell Death Discovery*. 2021;8(1):434. doi:10.1038/s41420-022-01212-0
36. Liu Z, Cao S, Chen Q, Fu F, Cheng M, Huang X. MicroRNA-132 promotes atherosclerosis by inducing mitochondrial oxidative stress-mediated ferroptosis. *Nan fang yi ke da xue xue bao*. 2022;42(1):143–149. doi:10.12122/j.issn.1673-4254.2022.01.18
37. Xiao FJ, Zhang D, Wu Y, et al. miRNA-17-92 protects endothelial cells from erastin-induced ferroptosis through targeting the A20-ACSL4 axis. *Biochem Biophys Res Commun*. 2019;515(3):448–454. doi:10.1016/j.bbrc.2019.05.147